

## Evaluation of fluoride-labeled boronophenylalanine-PET imaging for the study of radiation effects in patients with glioblastomas

Minoru Miyashita · Shin-Ichi Miyatake · Yoshio Imahori · Kunio Yokoyama · Shinji Kawabata · Yoshinaga Kajimoto · Masa-Aki Shibata · Yoshinori Otsuki · Mitsunori Kirihata · Koji Ono · Toshihiko Kuroiwa

Received: 14 April 2008 / Accepted: 28 May 2008 / Published online: 20 June 2008  
© Springer Science+Business Media, LLC. 2008

**Abstract** Here we demonstrate that differentiation between glioblastoma (GB) tumor progression (TP) and radiation necrosis (RN) can be achieved with fluoride-labeled boronoalanine positron emission tomography (F-BPA-PET). F-BPA-PET images were obtained from histologically verified 38 GB, 8 complete RN, and 5 RN cases with partial residual tumors. The lesion/normal (L/N) ratios for these groups were  $4.2 \pm 1.4$ ,  $1.5 \pm 0.3$ , and  $2.0 \pm 0.3$ , respectively. Ten GB patients underwent F-BPA-PET twice (once before and once after radiation treatment) due to enlargement of the original lesion or the development of new lesions post radiation. The L/N ratios of ten original site lesions had decreased by the second PET, and these lesions were revealed to be RN. In contrast, the L/N ratios of two lesions distant from the original site increased, and these lesions were revealed as cases of TP. Repeat PET imaging was found to be useful for evaluating changes in

GB-associated tumor activity with respect to the treatment received.

**Keywords** Boronophenylalanine · Glioblastoma · Positron emission tomography · Radiation necrosis

### Introduction

Glioblastoma (GB) is the most common primary malignant brain tumor. The treatment of patients with this pathology remains problematic. GB infiltrates into the normal brain parenchyma and is usually impossible to cure completely with surgical resection. Recently, new high-dose radiation therapies absorbed into the tumor tissue [e.g., boron neutron capture therapy (BNCT) and intensity-modulated radiotherapy (IMRT)] have been applied to treat patients with GB [1–4]. The efficacy of these treatments in eliciting clinical responses has been demonstrated in neuroimaging studies, in which lesions appear to have shrunk or the amount of peritumoral edema has decreased, and the associated clinical symptoms have likewise improved. Such radiation treatments and certain chemotherapeutic agents may alter the biological activity of tumor tissue, but it remains difficult to assess such changes.

It has been reported that high-dose, standard fractionated X-ray radiotherapy (XRT) has potential as a postoperative treatment for patients with supratentorial malignant gliomas [4]. Radiation necrosis (RN) was the most frequent adverse effect of radiation treatments, and excision of necrotic foci was required in some patients who had undergone standard XRT or IMRT [3, 4]. It remains important to evaluate the therapeutic effects of radiation therapy and chemotherapy on GB. Methods of treatment for RN and tumor progression (TP) differ substantially.

---

M. Miyashita · S.-I. Miyatake (✉) · K. Yokoyama · S. Kawabata · Y. Kajimoto · T. Kuroiwa  
Department of Neurosurgery, Osaka Medical College,  
2-7 Daigaku-machi, Takatsuki, Osaka 569-8686, Japan  
e-mail: neu070@poh.osaka-med.ac.jp

M.-A. Shibata · Y. Otsuki  
Department of Anatomy & Cell Biology, Osaka Medical  
College, Takatsuki, Osaka, Japan

Y. Imahori  
Cancer Intelligence Care System, Inc., Tokyo, Japan

M. Kirihata  
Department of Agriculture, Osaka Prefectural University,  
Sakai, Osaka, Japan

K. Ono  
Particle Radiation Oncology Research Center, Research Reactor  
Institute, Kyoto University, Kumatori, Osaka, Japan

Radiotherapy and chemotherapy combined with salvage surgery must be considered for TP, and RN may be treated initially, primarily using medical approaches (steroids, anticoagulants, vitamin E, etc.) [5–12]. Necrotic tissue should be excised when medical treatment means fail to control an increase in perifocal edema around a lesion. However, from a clinical perspective, it remains difficult to differentiate between these pathological conditions using ordinary neuroimaging technologies such as magnetic resonance imaging (MRI) and computed tomography (CT).

Here we examine and describe how to evaluate the biological activity of GB and how to differentiate radiation necrosis from GB tumor progression using positron emission tomography (PET) with fluoride-labeled boronophenylalanine (F-BPA) as a tracer.

## Materials and methods

### Patients

Thirty-eight patients with GB underwent an F-BPA-PET study. All patients were treated at the Department of Neurosurgery, Osaka Medical College, from January 2002 to December 2006, and received follow-up care until December 2007. Among these 38 patients, 19 had recurrent disease (those who had previously been treated with surgery and radiation treatments), and 19 were newly diagnosed with GB. All patients underwent surgery after being included in the study and the pathology results confirmed GB as the correct diagnosis after the patients underwent F-BPA-PET. In 10 of these 38 patients, F-BPA-PET was performed twice, i.e., once before treatment, including surgical resection followed by radiotherapy, and primarily with BNCT (this was defined as the first PET study); and once again after treatment, when enhanced lesions were enlarged at the original site (OS) or had newly appeared distant from the OS, as shown by follow-up gadolinium (Gd)-enhanced MRI. We defined the latter PET study as the second PET. We also categorized ten patients who underwent F-BPA-PET twice as belonging to a “twice-PET” group. In this latter group, following the second F-BPA-PET, seven patients received surgical resection of new or reappearing and enlarged lesions, and histological diagnoses were confirmed as RN or TP. The other lesions in the twice-PET group were followed monthly with Gd-MRI. If the lesions grew during the follow-up period, we considered them to constitute TP, and if they remained stable in size and shape, or decreased in size during the follow-up period (>4 months), we considered them to be RN. The profiles of the patients in this group are given in Table 1. Six lesions in four other patients, including patients with GB and other malignancies such as

metastatic brain tumors, were also given F-BPA-PET once only, when it was suspected that their intracranial lesions were RN, the sequelae of radiation therapy. All six lesions were histologically diagnosed as being either RN or RN in the main portion, with some residual tumor cells. We categorized these six lesions in these four patients as belonging to the “once-PET” group (Table 2).

### PET scan

All F-BPA-PET scans were performed at Nishijin Hospital, Kyoto, Japan. BPA was originally synthesized as described previously [13, 14] and the protocol for the PET measurements using a HEADTOME III (Shimadzu Co., Kyoto, Japan) has also been described elsewhere [15, 16]. Briefly, regional BPA incorporation into tumors and contralateral brain tissue (as a nontumorous control area) was measured on PET images after an intravenous injection of F-BPA at a dose of 37–55.5 MBq (1–1.5 mCi) per 10 kg of body weight. PET images were collected continuously for a 60-min period, for a total of 15 periods. The lesions on the PET images were confirmed using contrast-enhanced MRI performed at levels equivalent to those used for the PET imaging studies. To obtain quantitative measurements using Amide software (SourceForge, Inc.), oval regions of interest (ROIs) were placed on the tumors, including peak values in tumors of various sizes. At the corresponding level, the contralateral brain area was also chosen for ROI analysis. All of the macroscopically necrotic tumor areas observed on MRI were excluded when the ROIs were designated. We designated several ROIs from tumor-affected areas, and adopted regions with the highest values as representative ROIs. We determined each ROI at least 1 cm<sup>2</sup> at real area size.

### Statistical analysis

The L/N ratios of the 38 cases were analyzed using the Mann-Whitney *U* test, and the data from the first and second PET in the twice PET group were analyzed with the Wilcoxon matched-pair signed-rank test using StatView version 5.0 (SAS Institute, Inc.). We considered *p* values of less than 0.05 as statistically significant.

## Results

The L/N ratios of histologically verified GB cases and RN cases

We applied F-BPA-PET to examine 38 cases of histologically verified GB. The L/N ratio of these 38 cases was  $4.2 \pm 1.4$  (mean  $\pm$  standard deviation [SD]). We first compared

**Table 1** Patient characteristics who undergone F-BPA-PET two times (twice-PET group)

	Pre-Tx	L/N at first F-BPA-PET	Additional Tx	L/N at second F-BPA-PET	Result
Case 1		3.5	BNCT, XRT	1.9	RN (histological)
Case 2		2.6	BNCT, XRT	1.8	RN (clinical)
Case 3	XRT	3.3	BNCT	1.6	RN (histological)
Case 4		4.8	BNCT, XRT	1.8	RN (clinical)
Case 5		2.1	BNCT, XRT	1.4	RN with viable tumor cells (histological)
Case 6	SRS	5.0	BNCT, XRT	0.9	RN (histological)
Case 7 (OS)		4.3	BNCT, XRT × 2	1.9	RN (histological)
(RL)				3.1	TP (clinical)
Case 8 (OS)	XRT	2.6	BNCT	1.7	RN (clinical)
(RL)				2.9	TP (clinical)
Case 9	XRT	4.0	BNCT	2.1	RN with viable tumor cells (histological)
Case 10	XRT	3.7	BNCT	2.2	RN with viable tumor cells (histological)

BNCT: boron neutron capture therapy  
 Clinical: speculation by clinical course  
 Histological: histologically confirmed  
 OP: operation  
 OS: original site  
 RL: remote lesion  
 RN: radiation necrosis  
 SRS, SRT: stereotactic radiosurgery, or therapy  
 TP: tumor progression  
 Tx: treatment  
 XRT: X-ray radiation therapy

**Table 2** Patient characteristics, histologically verified RN (once-PET group)

Case	Pretreatment diagnosis	Treatment	L/N at F-BPA-PET after Tx	Histological diagnosis
Case 11	Meta	SRS × 2	1.4	Complete RN
Case 12	Meta	SRS × 2	2.2	RN with viable tumor cells
Case 13	GB	SRS, XRT	1.7	Complete RN
Case 14	GB	XRT	2.1	RN with viable tumor cells
Case 15	None*	XRT, BNCT × 2	1.5	Complete RN
Case 16	None*	XRT, BNCT × 2	1.4	Complete RN

*None*: No enhanced lesion was observed at intracranial before BNCT was performed for adenoductal carcinoma of parotid gland. Case 15 and 16 is the identical case but different lesions at frontla and temporal, respectively

the L/N ratios of newly diagnosed GB with those of recurrent GB cases. The L/N ratios of newly diagnosed GB were 2.1 to 7.1 ( $4.3 \pm 1.3$ ) and those of recurrent GB cases were 2.6 to 7.0 ( $3.9 \pm 1.4$ ). There was no significant difference between the L/N ratios these two groups ( $p = 0.16$ ), as shown in Fig. 1a. Next, we compared the L/N ratios of these histologically verified GB cases to those of histologically verified RN cases. The latter were composed of eight complete RN cases (four from the twice-PET group and four from the once-PET group), and five cases of primarily RN with partial residual tumor tissue (three from the

twice-PET group and two from the once-PET group). The L/N ratios were  $1.5 \pm 0.3$  and  $2.0 \pm 0.3$ , respectively. There were marked differences in the L/N ratios between GB cases (both the newly diagnosed and recurrent cases) and RN cases (both the complete necrosis cases and cases of necrosis in the main region, with partial residual tumor tissue, verified histologically) ( $p < 0.01$ ), as shown in Fig. 1b. There was a statistically significant difference in L/N ratios between necrosis cases and cases of necrosis in the main region, with partial residual tumor tissue, in all histologically verified cases ( $p = 0.03$ ) (Fig. 1a).

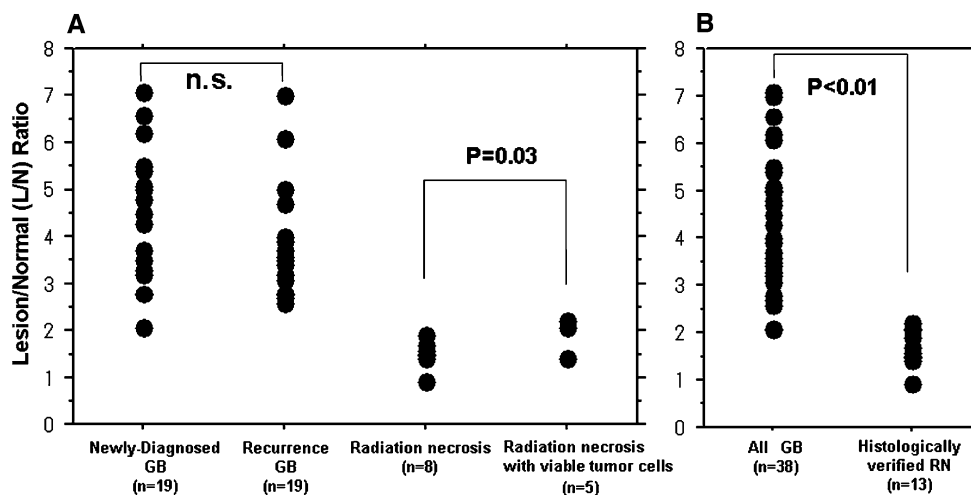


**Fig. 1** (a) The L/N ratios in histologically verified newly diagnosed and recurrent GB cases and in histologically verified RN cases with and without tumor components. The L/N ratios of newly diagnosed GB cases ranged from 2.1 to 7.1 ( $4.3 \pm 1.3$ ), and those of recurrent cases ranged from 2.6 to 7.0 ( $3.9 \pm 1.4$ ). There was no significant difference in the L/N ratio between newly diagnosed and recurrent GB cases ( $p = 0.16$ ). Histologically verified RN cases were composed of eight complete RN cases (four from the twice-PET group

and four from the once-PET group), and five primarily RN cases with partial residual tumors (one from the twice-PET group and two from the once-PET group). There was a significant difference in the L/N ratio for complete RN cases and primarily RN cases with partial residual tumors ( $p = 0.03$ ). (b) The L/N ratios in all GB cases and in histologically verified RN cases with and without tumor components. Significant statistical differences were observed in both groups ( $p < 0.01$ )

#### The L/N ratios of first versus second BPA-PET studies

In the twice PET group, we compared the L/N ratios between the first and the second PET studies. In all ten cases, BPA accumulation at OS in the second PET scan was lower than that in the first PET scan (Table 1 and Fig. 2). The L/N ratios in the first PET scan were 2.1 to 5.0 ( $3.5 \pm 0.9$ ). There was no significant difference between the L/N ratio of the first PET and that of all 38 cases ( $p = 0.34$ ). In the second PET, the L/N ratio of the ten lesions at OS was 0.9 to 2.2 ( $1.7 \pm 0.3$ ). There was a significant difference between the L/N ratios of the ten lesions at OS in the second PET scan and those in the first PET scan ( $p < 0.01$ ), as shown in Fig. 2. All ten lesions at OS were judged as RN. Seven of these lesions were histologically verified as RN, and the remaining three were considered to be RN based on the clinical course. Moreover, the L/N ratios of the lesions judged as RN were statistically different from those of cases of total GB and also from those of cases of recurrent GB ( $p < 0.01$ ). There was no significant difference between the L/N ratio of histological RN cases ( $n = 13$  in Tables 1 and 2) and that of cases of clinical RN ( $n = 3$  in Table 1) ( $p = 0.89$ ).

On the other hand, the L/N ratios in the second PET study obtained from the two lesions distant from the OS were 2.9 and 3.1 (cases 7 and 8 in Table 1, and open triangles in Fig. 2). These lesions were not verified as TP by histological examination, whereas the clinical courses of both lesions suggested a high possibility of TP, because follow-up MRI showed rapid growth of both lesions,

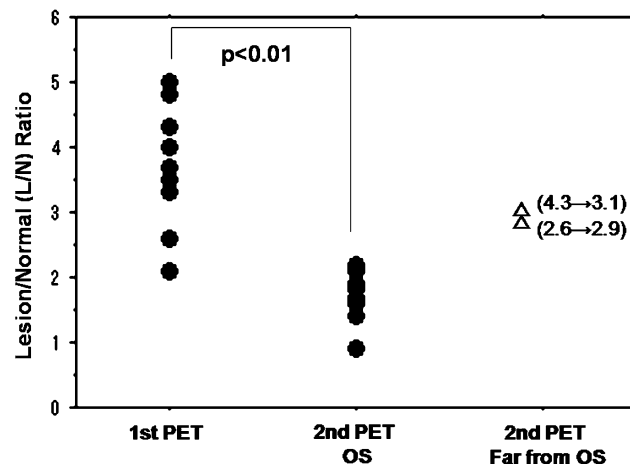


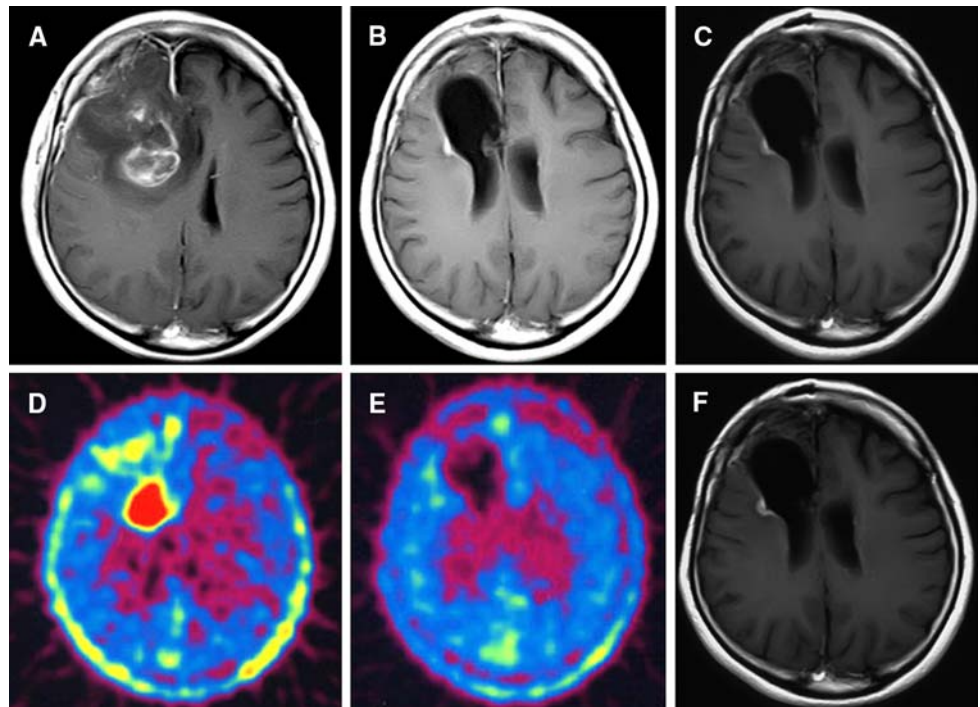
**Fig. 2** Comparison of the L/N ratios in the GB of the first PET with that of the second PET. Filled circles and open triangles express the L/N ratios at the original site and remote lesions, respectively. Filled circles on the second PET were all cases of RN (seven cases histologically verified, and three cases clinically suspected). Open triangles indicate the non-OS L/N ratio and that for lesions clinically considered as TP. Statistical significance was observed in the L/M ratios between the first PET and the second PET at OS ( $p < 0.01$ )

whereas the lesions at OS of the same cases were stable in size and judged as RN.

#### Illustrative cases

**Case 6:** GB treated with surgical resection and BNCT (Table 1 and Fig. 3)

**Fig. 3** A representative case (case 6): GB treated by surgical resection and BNCT. Glioblastoma treated by surgical resection followed by BNCT and 40 Gy conventional XRT. (a) Gd-MRI taken just prior to the second surgery. (b, c) Periodic follow-up MRI. (d) First PET, taken just prior to the second surgery, showing high F-BPA accumulation; L/N 5.0. (e) Second PET, taken 6 months after BNCT. The L/N ratio was 0.9 in this PET, suggesting radiation necrosis of the enhancement-positive lesion. (f) No enlargement of this enhanced lesion was recognized in follow-up MRI for 10 months after the last surgery



This is a patient with a glioma in the right frontal lobe. Surgical resection was applied, and the histological diagnosis was anaplastic oligodendroglioma. After the operation, adjuvant therapy was administered (chemotherapy with nimustin, procarbazine, and vincristin and stereotactic radiosurgery (SRS) for the enhanced lesion). Eight months after the final chemotherapy treatment, local recurrence was observed on MRI. The patient was referred to our clinic, and the first PET suggested tumor recurrence (L/N ratio 5.0, Fig. 3a, d). The second surgical resection was performed, and the histological diagnosis of the surgical specimen was GB with oligodendroglioma component. After the second operation, BNCT was performed, with a minimum tumor dose of 37.3 Gy-Eq: (Gray-equivalent), i.e., a biologically equivalent X-ray dose that can yield effects equivalent to total particle radiation with BNCT; also in addition, the maximum normal tissue dose of 8.34 Gy-Eq and conformal XRT was added to treat the deep lesion (40 Gy). Six months after the second operation, a locally enhanced lesion with perifocal edema was recognized on MRI, and the patient underwent a second PET. The L/N ratio was 0.9 in the second PET study, suggesting RN of the enhanced lesion (Fig. 3b, e). No enlargement of the enhanced lesion was obtained in the follow-up Gd-enhanced MRI at 10 months, and a clinical diagnosis of radiation necrosis was given (Fig. 3c, f). The patient wanted histological confirmation that the lesion was truly RN, and therefore we performed a surgical biopsy. The histological diagnosis was pure necrosis; no tumor cells were found.

*Case 7:* GB recurrence treated with surgical resection, BNCT, and XRT twice (Table 1 and Fig. 4)

This is a patient with glioblastoma in the right parietal lobe. The first surgical resection was performed and the histological diagnosis was GB. Before first resection, MRI and F-BPA-PET were carried out (Fig. 4a, b). The L/N ratio of the OS in the first PET study was 4.3. After gross total resection, BNCT was performed with a minimum tumor dose of 50.5 Gy-Eq, and a maximum normal tissue dose of 13.3 Gy-Eq, and for a deep lesion, XRT (30 Gy) was added. Ten months after BNCT, a new lesion appeared at the bottom of the cavity where the previous lesion had been removed, and this lesion had invaded to the splenium at the opposite side. Additional 50 Gy XRT was applied with two opposed right-left beams, followed by chemotherapy with Temozolomide; this approach controlled growth of the lesion for another 8 months. After this period of stabilization, the enhanced lesion at the OS was enlarged and some enhanced lesions far from the OS were detected in follow-up MRI (Fig. 4c, d). The patient exhibited left hemiparesis due to perifocal edema of the enhanced lesion at the OS. A second surgical resection was performed on the OS lesion to control the perifocal edema. Prior to the second operation, a second PET study was carried out (Fig. 4e, f). The L/N ratio of the lesion at the OS was 1.9. On the other hand, the L/N ratio of the remote enhanced lesion was 3.1, and we arrived at a diagnosis of TP due to cerebrospinal fluid dissemination. The surgical specimen from the second operation showed radiation necrosis (Fig. 4g). The OS lesion was not enlarged on follow-up MRI, but the remote lesion rapidly enlarged.

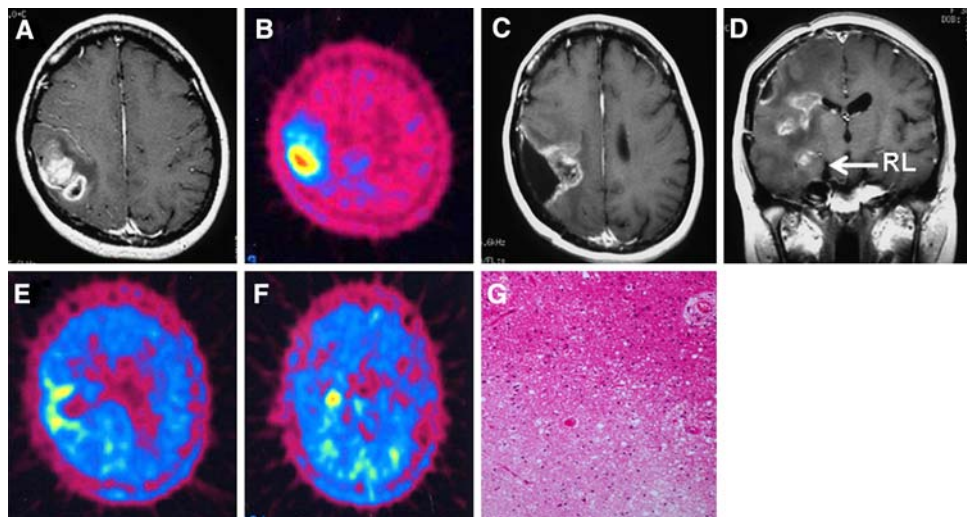


**Fig. 4** A representative case (case 7): GB treated with surgical resection, BNCT, and XRT  $\times$  2. (a, b) Initial Gd-MRI and F-BPA-PET (First PET) just prior to the first surgery; the L/N ratio was 4.3. (c, d) Follow-up MRI 1.5 years after BNCT and XRT  $\times$  2 prior to the second surgery. The enhanced lesion of OS lesion was enlarged, and a remote lesion (RL), which was considered to have disseminated, was

observed. (e, f) Second PET was performed, and the L/N ratio of the OS lesion was 1.9, which suggested radiation necrosis of the enhancement-positive lesion; the L/N ratio of the RL was 3.1, which on this PET study was suggestive of tumor progression. (g) A second surgical specimen was confirmed histologically to be RN

## Discussion

New modalities for the treatment of malignant gliomas (MG), and primarily of GB, have recently been introduced. In addition, new chemotherapeutic agents such as Temozolomide are being developed for the treatment of MG [17]. The main approach to the adjuvant treatment of MG remains radiotherapy, and this approach is also advancing. To date, not only conventional XRT and SRS, but also new brachytherapies such as gliasite [18] and IMRT, a particle radiation modality, have been developed to administer highly absorbed doses to tumorous tissue with high conformity [1, 3, 19]. In addition, BNCT, a tumor-selective targeting particle radiation treatment, has been used for the treatment of malignant brain tumors [2, 20, 21]. These new modalities are steadily improving the results of MG treatment, although local high-dose radiation itself increases the possibility of RN. Even BNCT, if applied in recurrent cases, carries the risk of RN due to previous XRT exposure, as shown in Table 1.

It is important to differentiate between RN and TP when determining the optimal radiation dose for high-dose radiation studies such as BNCT, IMRT, and particle radiation therapies. If we consider a lesion to be TP, the radiation dose should be increased, whereas if it is deemed to be a case of RN, the radiation dose should be decreased at the next step of a radiation study. It is crucial to distinguish correctly between RN and TP, because the appropriate treatment differs for each pathological condition after diagnosis. If an incorrect diagnosis leads to the

application of the wrong treatment, the treatment itself may decrease the patients' quality of life or even shorten survival. In many cases, earlier diagnosis may also lead to a better outcome.

A number of modalities for differentiating between RN and malignant tumor recurrence have been studied, including thallium-single photon emission computed tomography (SPECT) [22] and magnetic resonance spectroscopy (MRS) [23]. Among such approaches, PET imaging has undergone rigorous scrutiny as it allows for the direct analysis of tissue metabolism. In some patients with suspected RN who underwent F-BPA-PET and surgery, we applied MRS mapping. Moreover, in some of our cases, MRS and PET yielded the same results (RN), while in other cases, no lactate and lipid peaks, which are indicators of RN on MRS, correctly, while F-BPA-PET suggested RN, and histological examination confirmed the diagnosis of RN (data not shown).

In addition, a number of different tracers have been used for PET imaging to detect malignant tumors. Fluorodeoxyglucose (FDG) has been used and studied in numerous tumor types [24]. The brain shows high sugar metabolism, and FDG-PET reveals a very high metabolic background in the normal brain. Moreover, FDG accumulates well in cases of inflammation [25]. However, inflammatory cells commonly infiltrate at the RN border as well as in normal brain tissue [21, 26]. Therefore, it remains rather difficult to apply FDG-PET for discriminating between RN and TP [27]. It has been reported that, in some RN cases, FDG accumulates well in the absence of evidence of tumor

recurrence [28]. PET imaging using amino acids as tracers is promising for the detection of malignant tumors in the brain, because the background activity of protein metabolism in the brain is rather low in comparison with that of sugar.  $^{11}\text{C}$ -labeled methionine (MET) has been used as a tracer for amino-PET [29, 30]. This tracer has been used for analyzing metabolism in malignant brain tumors [29, 30] as well as for differentiating between RN and TP [30]. A known potential disadvantage of  $^{11}\text{C}$ -labeled substances such as methionine is that, due to the short half-life of the tracer, they are unavailable to PET centers without a cyclotron [31]. On the other hand,  $^{18}\text{F}$ -labeled substances have a longer half-life. We confirmed that the addition of boron to phenylalanine at the phenyl radical improves biodistribution over that achieved with naïve phenylalanine. Phenylalanine itself tends to become trapped at the liver if it is administered systemically. We speculate that the addition of boron at the phenyl radical in phenylalanine inhibits the nonspecific uptake of the tracer in the liver in comparison with that of naïve phenylalanine [32, 33]. Originally we and others undertook F-BPA-PET studies for the purpose of BNCT [32–34]. One of the present authors (Y.I.) reported that the accumulation of this tracer correlates well with clinical malignancy and correlates inversely with patient survival [15, 16, 32, 33]. In addition, the accumulation of this tracer may enable differentiation between RN and TP, as described here. Here, a marked difference between the L/N ratios of GB and RN was observed; the lowest L/N ratio in GB listed here was 2.1, and the highest L/N ratio was 2.2, in cases primarily consisting of RN with a partial tumor residue. Therefore, it remains difficult to distinguish between RN and TP in all cases, especially when only a single F-BPA-PET evaluation is performed.

Finally, it should be kept in mind that, even in patients with L/N ratios of  $<2.0$ , viable or recurrent tumor cells may be present in the tissue. We identified some tumor cells in the majority of necrotic tissues when necrotic tissue was removed, even in patients with L/N ratios of less than 2.0, as shown in Table 1. The majority of tissues can only be deemed necrotic if the L/N ratio is below 2.0. In such cases, the RN must be removed and/or treated with various therapies such as steroids, anticoagulants, hyperbaric oxygenation, and vitamin E.

## Conclusions

There were significant differences between GB tumor progression and radiation necrosis in the L/N ratios observed on F-BPA-PET imaging. An L/N ratio on F-BPA-PET of greater than 2.5 is strongly suggestive of TP, and an L/N ratio of less than 2.0 suggests a high possibility of RN.

**Acknowledgments** This work was partly supported by a Grant-in-Aid for Scientific Research (B) (16390422, 19390385) from the Japanese Ministry of Education, Culture, Sports, Science, and Technology to Shin-Ichi Miyatake. This work was also supported in part by the Takeda Science Foundation for Osaka Medical College. We are also grateful to Mr. Horii at Nishijin Hospital for technical support with the PET study.

## References

- Narayana A, Yamada J, Berry S, Shah P, Hunt M, Gutin PH, Leibel SA (2006) Intensity-modulated radiotherapy in high-grade gliomas; clinical and dosimetric results. *Int J Radiat Oncol Biol Phys* 64:892–897
- Miyatake S, Kawabata S, Kajimoto Y, Aoki A, Yokoyama K, Yamada M, Kuroiwa T, Tsuji M, Imahori Y, Kirihata M, Sakurai Y, Masunaga S, Nagata K, Maruhashi A, Ono K (2005) Modified boron neutron capture therapy for malignant gliomas performed using epithermal neutron and two boron compounds with different accumulation mechanisms: an efficacy study based on findings on neuroimages. *J Neurosurg* 103:1000–1009
- Iuchi T, Hatano K, Narita Y, Kodama T, Yamaki T, Osato K (2006) Hypofractionated high-dose irradiation for the treatment of malignant astrocytomas using simultaneous integrated boost technique by IMRT. *Int J Radiat Oncol Biol Phys* 64:1317–1324
- Tanaka M, Ino Y, Nakagawa K, Tago M, Todo T (2005) High-dose conformal radiotherapy for supratentorial malignant glioma: a historical comparison. *Lancet Oncol* 6:953–960
- Burger P, Boyko O (1991) The pathology of central nervous system radiation injury. In: Gutin PH, Leibel SA, Sheline GE (eds) *Radiation injury to the nervous system*. Raven Press, New York, pp 191–208
- Delanian S, Balla-Mekias S, Lefaix JL (1999) Striking regression of chronic radiotherapy damage in a clinical trial of combined pentoxifylline and tocopherol. *J Clin Oncol* 17:3283–3290
- DiLorenzo N, Nolletti A, Palma L (1978) Late cerebral radionecrosis. *Surg Neurol* 10:281–290
- Eyster EF, Nielsen SL, Sheline GE, Wilson CB (1974) Cerebral radiation necrosis simulating a brain tumor. Case report. *J Neurosurg* 40:267–271
- Glantz MJ, Burger PC, Friedman AH, Radtke RA, Massey EW, Schold SC Jr (1994) Treatment of radiation-induced nervous system injury with heparin and warfarin. *Neurology* 44:2020–2027
- Kusske JA, Williams JP, Garcia JH, Pribram HW (1976) Radiation necrosis of the brain following radiotherapy of extracerebral neoplasms. *Surg Neurol* 6:15–20
- Martins AN, Johnston JS, Henry JM, Stoffel TJ, Di Chiro G (1977) Delayed radiation necrosis of the brain. *J Neurosurg* 47:336–345
- Rizzoli HV, Pagnanelli DM (1984) Treatment of delayed radiation necrosis of the brain. A clinical observation. *J Neurosurg* 60:589–594
- Ishiwata K, Ido T, Mejia AA, Ichihashi M, Mishima Y (1991) Synthesis and radiation dosimetry of 4-borono-2-[ $^{18}\text{F}$ ]fluoro-D L-phenylalanine: a target compound for PET and boron neutron capture therapy. *Int J Rad Appl Instrum [A]* 42:325–328
- Mishima Y, Imahori Y, Honda C, Hiratsuka J, Ueda S, Ido T (1997) In vivo diagnosis of human malignant melanoma with positron emission tomography using specific melanoma-seeking  $^{18}\text{F}$ -DOPA analogue. *J Neurooncol* 33:163–169
- Imahori Y, Ueda S, Ohmori Y, Kusuki T, Ono K, Fujii R, Ido T (1998) Fluorine-18-labeled fluoroboronophenylalanine PET in patients with glioma. *J Nucl Med* 39:325–333

16. Takahashi Y, Imahori Y, Mineura K (2003) Prognostic and therapeutic indicator of fluoroboronophenylalanine positron emission tomography in patients with gliomas. *Clin Cancer Res* 9:5888–5895
17. Stupp R, Mason WP, van den Bent MJ, Weller M, Fisher B, Taphoorn MJ, Belanger K, Brandes AA, Marosi C, Bogdahn U, Curschmann J, Janzer RC, Ludwin SK, Gorlia T, Allgeier A, Lacombe D, Cairncross JG, Eisenhauer E, Mirimanoff RO (2005) Radiotherapy plus concomitant and adjuvant temozolomide for glioblastoma. *N Engl J Med* 352:987–996
18. Gabayan AJ, Green SB, Sanan A, Jenrette J, Schultz C, Papagikos M, Tatter SP, Patel A, Amin P, Lustig R, Bastin KT, Watson G, Burri S, Stea B (2006) GliaSite brachytherapy for treatment of recurrent malignant gliomas: a retrospective multi-institutional analysis. *Neurosurgery* 58:701–709; discussion 701–709
19. Hermanto U, Frija EK, Lii MJ, Chang EL, Mahajan A, Woo SY (2007) Intensity-modulated radiotherapy (IMRT) and conventional three-dimensional conformal radiotherapy for high-grade gliomas: does IMRT increase the integral dose to normal brain? *Int J Radiat Oncol Biol Phys* 67:1135–1144
20. Kawabata S, Miyatake S, Kajimoto Y, Kuroda Y, Kuroiwa T, Imahori Y, Kirihata M, Sakurai Y, Kobayashi T, Ono K (2003) The early successful treatment of glioblastoma patients with modified boron neutron capture therapy. Report of two cases. *J Neurooncol* 65:159–165
21. Miyatake S, Kuroiwa T, Kajimoto Y, Miyashita M, Tanaka H, Tsuji M (2007) Fluorescence of non-neoplastic, MRI-enhancing tissue by 5-aminolevulinic acid: report of 3 cases. *Neurosurgery* 61:E1101–E1103
22. Sonoda Y, Kumabe T, Takahashi T, Shirane R, Yoshimoto T (1998) Clinical usefulness of <sup>11</sup>C-MET PET and <sup>201</sup>Tl SPECT for differentiation of recurrent glioma from radiation necrosis. *Neurol Med Chir (Tokyo)* 38:342–347; discussion 347–348
23. Rock JP, Scarpace L, Hearshen D, Gutierrez J, Fisher JL, Rosenblum M, Mikkelsen T (2004) Associations among magnetic resonance spectroscopy, apparent diffusion coefficients, and image-guided histopathology with special attention to radiation necrosis. *Neurosurgery* 54:1111–1117; discussion 1117–1119
24. Shankar LK, Hoffman JM, Bacharach S, Graham MM, Karp J, Lammertsma AA, Larson S, Mankoff DA, Siegel BA, Van den Abbeele A, Yap J, Sullivan D (2006) Consensus recommendations for the use of <sup>18</sup>F-FDG PET as an indicator of therapeutic response in patients in National Cancer Institute Trials. *J Nucl Med* 47:1059–1066
25. Meller J, Sahlmann CO, Scheel AK (2007) <sup>18</sup>F-FDG PET and PET/CT in fever of unknown origin. *J Nucl Med* 48:35–45
26. Burger PC, Mahley MS Jr, Dudka L, Vogel FS (1979) The morphologic effects of radiation administered therapeutically for intracranial gliomas: a postmortem study of 25 cases. *Cancer* 44:1256–1272
27. Wang SX, Boethius J, Ericson K (2006) FDG-PET on irradiated brain tumor: ten years' summary. *Acta Radiol* 47:85–90
28. Hung GU, Tsai SC, Lin WY (2005) Extraordinarily high F-18 FDG uptake caused by radiation necrosis in a patient with nasopharyngeal carcinoma. *Clin Nucl Med* 30:558–559
29. Ceyskens S, Van Laere K, de Groot T, Goffin J, Bormans G, Mortelmans L (2006) [<sup>11</sup>C]methionine PET, histopathology, and survival in primary brain tumors and recurrence. *AJNR Am J Neuroradiol* 27:1432–1437
30. Tsuyuguchi N, Takami T, Sunada I, Iwai Y, Yamanaka K, Tanaka K, Nishikawa M, Ohata K, Torii K, Morino M, Nishio A, Hara M (2004) Methionine positron emission tomography for differentiation of recurrent brain tumor and radiation necrosis after stereotactic radiosurgery – in malignant glioma. *Ann Nucl Med* 18:291–296
31. Laverman P, Boerman OC, Corstens FH, Oyen WJ (2002) Fluorinated amino acids for tumour imaging with positron emission tomography. *Eur J Nucl Med Mol Imaging* 29:681–690
32. Imahori Y, Ueda S, Ohmori Y, Sakae K, Kusuki T, Kobayashi T, Takagaki M, Ono K, Ido T, Fujii R (1998) Positron emission tomography-based boron neutron capture therapy using boronophenylalanine for high-grade gliomas: part I. *Clin Cancer Res* 4:1825–1832
33. Imahori Y, Ueda S, Ohmori Y, Sakae K, Kusuki T, Kobayashi T, Takagaki M, Ono K, Ido T, Fujii R (1998) Positron emission tomography-based boron neutron capture therapy using boronophenylalanine for high-grade gliomas: part II. *Clin Cancer Res* 4:1833–1841
34. Joensuu H, Kankaanranta L, Seppala T, Auterinen I, Kallio M, Kulvik M, Laakso J, Vahatalo J, Kortelainen M, Kotiluoto P, Seren T, Karila J, Brander A, Jarviluoma E, Ryyanen P, Paetau A, Ruokonen I, Minn H, Tenhunen M, Jaaskelainen J, Farkkila M, Savolainen S (2003) Boron neutron capture therapy of brain tumors: clinical trials at the Finnish facility using boronophenylalanine. *J Neurooncol* 62:123–134